

# Frequency combinations in the magnetoresistance oscillations spectrum of a linear chain of coupled orbits with a high scattering rate

David Vignolles<sup>1</sup>, Alain Audouard<sup>1</sup>, Vladimir N. Laukhin<sup>2,3</sup>, Jérôme Béard<sup>1</sup>, Enric Canadell<sup>3</sup>, Nataliya G. Spitsina<sup>4</sup> and Eduard B. Yagubskii<sup>4</sup>

<sup>1</sup> Laboratoire National des Champs Magnétiques Pulsés <sup>a</sup>, 143 avenue de Rangueil, 31400 Toulouse, France.

<sup>2</sup> Institució Catalana de Recerca i Estudis Avançats (ICREA) 08210 Barcelona, Spain.

<sup>3</sup> Institut de Ciència de Materials de Barcelona, CSIC, Campus de la UAB, 08193, Bellaterra, Spain

<sup>4</sup> Institute of Problems of Chemical Physics, RAS, 142432 Chernogolovka, MD, Russia

Received: March 9, 2007/ Revised version: date

**Abstract.** The oscillatory magnetoresistance spectrum of the organic metal (BEDO)<sub>5</sub>Ni(CN)<sub>4</sub>·3C<sub>2</sub>H<sub>4</sub>(OH)<sub>2</sub> has been studied up to 50 T, in the temperature range from 1.5 K to 4.2 K. In high magnetic field, its Fermi surface corresponds to a linear chain of quasi-two-dimensional orbits coupled by magnetic breakdown (MB). The scattering rate consistently deduced from the data relevant to the basic  $\alpha$  and the MB-induced  $\beta$  orbits is very large which points to a significant reduction of the chemical potential oscillation. Despite of this feature, the oscillations spectrum exhibits many frequency combinations. Their effective masses and (or) Dingle temperature are not in agreement with either the predictions of the quantum interference model or the semiclassical model of Falicov and Stachowiak.

**PACS.** 71.18.+y Fermi surface: calculations and measurements; effective mass, g factor – 71.20.Rv Polymers and organic compounds – 72.20.My Galvanomagnetic and other magnetotransport effects

## 1 Introduction

According to band structure calculations [1], the Fermi surface (FS) of many quasi-two-dimensional (q-2D) organic metals with two charge carriers per unit cell originates from one ellipsoidal hole tube whose area is therefore equal to that of the first Brillouin zone (FBZ) area. In the extended zone scheme, this tube can go over the FBZ boundaries along either one or two directions leading to FS with different topologies. Due to gaps opening at the crossing points, the resulting FS is composed of a q-2D tube and a pair of q-1D sheets in the former case while, in the second case, compensated electron and hole tubes are observed. In high enough magnetic field, both of these FS's can be regarded as networks of orbits coupled by magnetic breakdown (MB) which can therefore be classified according to two types: the well known linear chain of coupled orbits [2,3] and the network of compensated electron and hole orbits [4], respectively.

In both cases, oscillatory magnetoresistance spectra exhibit frequencies which are linear combinations of a few basic frequencies. Magnetoresistance oscillations in linear chains of coupled orbits have been studied, in particular in the case of the compound  $\kappa$ -(BEDT-TTF)<sub>2</sub>Cu(NCS)<sub>2</sub> [5,6]. In addition to the frequencies linked to the q-2D  $\alpha$  orbit and the MB-induced  $\beta$  orbit (which corresponds to the hole tube from which the FS is built) many combinations that can be attributed to MB ( $\beta + \alpha$ ,  $\beta + 2\alpha$ , etc.)

are observed in the Fourier spectra. Other Fourier components such as  $\beta - \alpha$  [5] or  $\beta - 2\alpha$  [6] are also detected. These latter frequencies are currently interpreted on the basis of quantum interference (QI), although they are also observed in de Haas-van Alphen (dHvA) oscillations spectra [7,8,9].

According to theoretical studies, both the field-dependent modulation of the density of states due to MB [2,3,10] and the oscillation of the chemical potential [11] can also induce frequency combinations in magnetoresistance and dHvA oscillatory spectra. Nevertheless, the respective influence of each of these contributions on the magnetoresistance and dHvA spectra remains to be determined. Among them, the oscillation of the chemical potential can be strongly reduced at high temperature [11] and (or) for high scattering rate [12]. Nevertheless, small effective masses are required in these cases in order to observe quantum oscillations with a high enough signal-to-noise ratio, at low enough magnetic field.

In this paper, we report on magnetoresistance experiments up to 50 T on (BEDO)<sub>5</sub>Ni(CN)<sub>4</sub>·3C<sub>2</sub>H<sub>4</sub>(OH)<sub>2</sub> of which, according to band structure calculations [13], the FS can be regarded as a linear chain of coupled orbits. It is shown that the crystals studied meet the above cited requirements, namely, high scattering rates and low effective masses. Nevertheless, many frequency combinations are observed in the oscillatory spectra.

<sup>a</sup> UMR 5147: Unité Mixte de Recherche CNRS - Université

## 2 Experimental

The studied crystals, labelled #1 and #2 in the following, were synthesized by the electrocrystallization technique reported in Ref. [13]. They are roughly parallelepiped-shaped with approximate dimensions ( $0.6 \times 0.3 \times 0.1$ ) mm<sup>3</sup>, the largest faces being parallel to the conducting *ab* plane. Electrical contacts were made to the crystals using annealed Pt wires of 20  $\mu$ m in diameter glued with graphite paste. Alternating current (10 to 100  $\mu$ A, 20 kHz) was injected parallel to the *c*\* direction (interlayer configuration). Magnetoresistance measurements were performed in pulsed magnetic field of up to 50 T with pulse decay duration of 0.78 s, in the temperature range (1.5 - 4.2) K. A lock-in amplifier with a time constant of 30  $\mu$ s was used to detect the signal across the potential leads.

## 3 Results and discussion

As reported in Figure 1, the zero-field interlayer resistance of the two studied crystals monotonically decreases as the temperature decreases down to 1.5 K, as it is the case for the in-plane resistance [13]. The resistance ratio between room temperature and 4.2 K (RR) is 39 and 36 for crystal #1 and #2, respectively. These values (which are higher than for the in-plane resistance data [13] for which RR = 16) are much lower than those reported for other compounds with similar FS such as  $\kappa$ -(BEDT-TTF)<sub>2</sub>Cu(NCS)<sub>2</sub> [14], (BEDT-TTF)<sub>4</sub>[Ni(dto)<sub>2</sub>] [15] and  $\kappa$ -(BEDT-TTF)<sub>2</sub>I<sub>3</sub> [16], namely, RR  $\approx$  200, 400 and 8000, respectively.

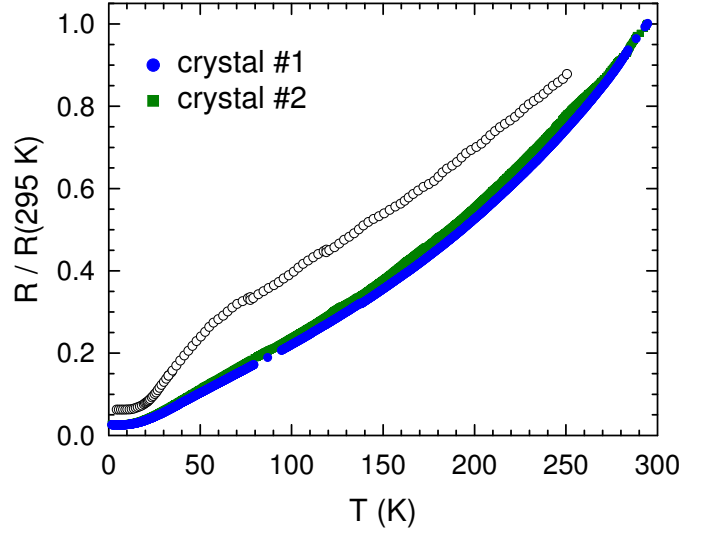


**Fig. 1.** Temperature dependence of the normalized interlayer resistance of crystals #1 and #2 (solid symbols). Open symbols stand for the in-plane resistance data of Ref. [13].

Magnetoresistance data of the two crystals yield consistent results. In the following, we mainly focus on the data recorded from crystal #1 which was more extensively studied. As generally observed for clean linear chains of coupled orbits, many Fourier components are observed in the oscillatory magnetoresistance spectra of which the frequencies are linear combinations of those linked to the closed  $\alpha$  and the MB-induced  $\beta$  orbits (see Figure 2 and Table 1). The measured value of  $F_\beta$  is in good agreement with the expected value for an orbit area equal to that of the FBZ. Indeed, according to crystallographic data at room temperature [13],  $F_\beta$  should be equal to 3839 T.  $F_\alpha$  corresponds to a cross section area of 14.4 percent of the room temperature FBZ area. It is smaller than the value predicted by band structure calculations [13], namely 20.8 percent of the FBZ area. Nevertheless, the obtained value is very close to those reported for several compounds with

**Table 1.** Frequencies and effective masses (in  $m_e$  units) linked to the various Fourier components (index  $i$  of Eqs. 1 to 3) appearing in Figure 2.

$i$	$F_i$ (T)	$m_i^*$
$\alpha$	$552 \pm 3$	$1.15 \pm 0.05$
$2\alpha$	$1104 \pm 12$	$2.30 \pm 0.08$
$\beta - 2\alpha$	$2720 \pm 40$	$0.3 \pm 0.3$
$\beta - \alpha$	$3278 \pm 9$	$1.68 \pm 0.05$
$\beta$	$3837 \pm 24$	$1.80 \pm 0.15$
$\beta + \alpha$	$4388 \pm 12$	$3.55 \pm 0.15$

similar FS such as  $\kappa$ -(BEDT-TTF) $_2$ Cu(NCS) $_2$  [17] and (BEDT-TTF) $_2$ I $_3$  [18] for which the  $\alpha$  orbit area amounts to 15 percent of the FBZ area. Band structure calculations often lead to an overestimation of the area associated with the  $\alpha$  orbit for  $\beta^n$ -BEDO salts with this type of FS (see for instance ref. [19]). Because of the scarcity of results it is not clear at this time if this discrepancy is intrinsic to the theoretical approach used to calculate the FS when considering BEDO donors, or due to an unusual thermal contraction behavior of these salts leading to larger changes than for similar sulfur-containing donors. However this quantitative aspect is only of marginal importance for the present study.

With regard to the amplitude of the Fourier components appearing in Figure 2, the most striking feature is the small amplitude of the  $\beta$  component with respect to e.g. that attributed to the MB-induced  $\beta + \alpha$  orbit. Indeed, in the framework of the semiclassical model (see the discussion below), the damping factors of the amplitude

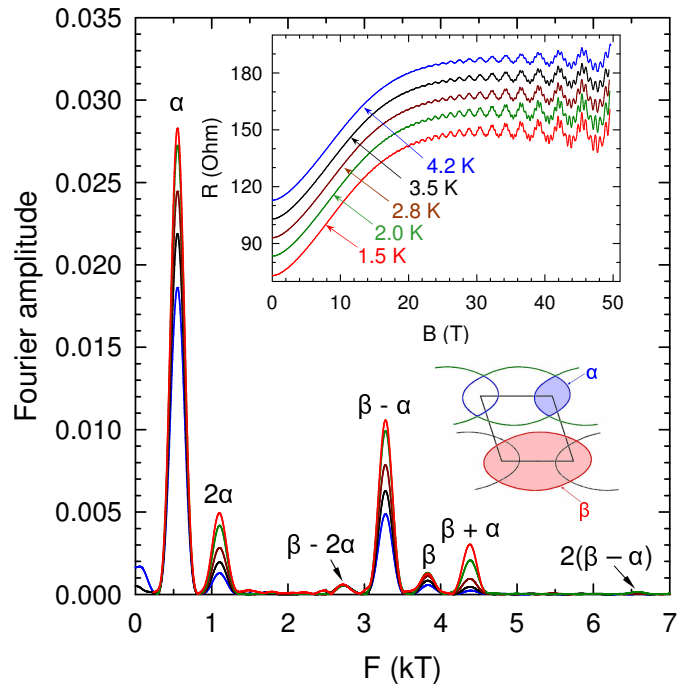


**Fig. 2.** Fourier spectra deduced from the magnetoresistance data displayed in the upper inset, in the field range 32 T - 49.4 T. In this inset, the magnetoresistance curves are shifted up by 10 ohms from each other for clarity. The lower inset displays the Fermi surface deduced from band structure calculations [13].

of this latter component are smaller than that related to  $\beta$ . The relatively large amplitude of the  $\beta - \alpha$  component can also be noticed. We have checked by changing the direction of the magnetic field with respect to the crystalline axes that these features, which are also observed in other organic metals with similar FS [5,19], are not due to spin-zero phenomenon<sup>1</sup>.

<sup>1</sup> A change by a few degrees of the magnetic field direction with respect to the normal to the conducting plane leads to a steep (certainly due to the measured high Dingle temperature, see below) decrease of both the  $\beta - \alpha$ ,  $\beta$  and  $\beta + \alpha$  Fourier components's amplitude.

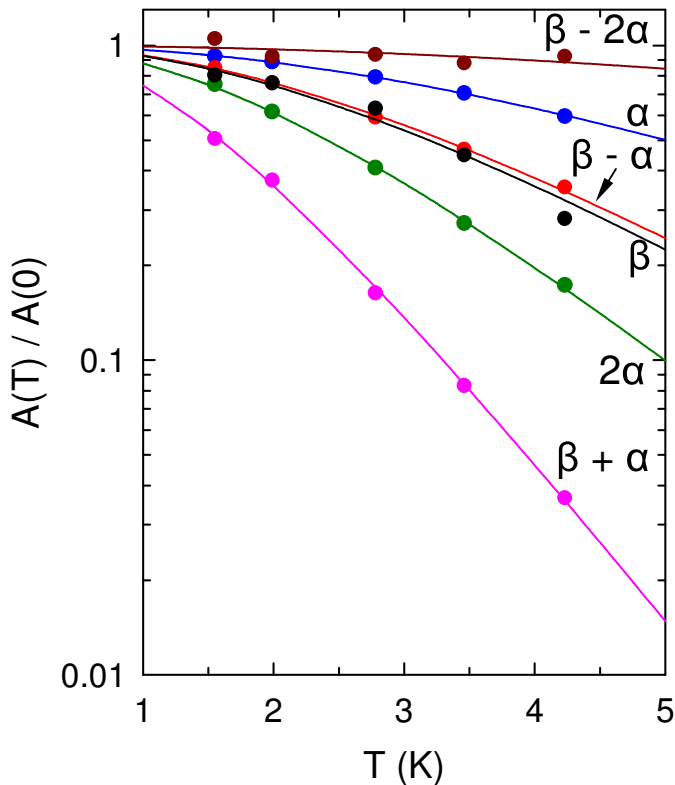


**Fig. 3.** Temperature dependence of the amplitude of the various Fourier components observed in Figure 2, for a mean magnetic field value of 38 T. Solid lines are best fits to Eq. 1.

Let us consider in more detail the field and temperature dependence of the amplitude of the Fourier components observed in Figure 2. In the framework of the Lifshits-Kosevich (LK) model, the oscillatory magnetoresistance can be written as:

$$\frac{R(B)}{R_{background}} = 1 + \sum_i A_i \cos[2\pi(\frac{F_i}{B} - \gamma_i)] \quad (1)$$

where  $R_{background}$  is the monotonic part of the field-dependent resistance  $R(B)$  and  $\gamma_i$  is a phase factor. The amplitude of the Fourier component with the frequency  $F_i$  is given by  $A_i \propto R_{T_i} R_{D_i} R_{MB_i} R_{S_i}$ , where the spin damping factor ( $R_{S_i}$ ) depends only on the direction of the

magnetic field with respect to the conducting plane. The thermal, Dingle and MB damping factors are respectively given by:

$$R_{T_i} = \frac{\alpha T m_i^*}{B \sinh[\alpha T m_i^*/B]} \quad (2)$$

$$R_{D_i} = \exp[-\alpha T_D m_i^*/B] \quad (3)$$

$$R_{MB_i} = \exp(-\frac{t_i B_{MB}}{2B}) [1 - \exp(-\frac{B_{MB}}{B})]^{b_i/2} \quad (4)$$

where  $\alpha = 2\pi^2 m_e k_B / e\hbar$  ( $\simeq 14.69$  T/K),  $m_i^*$  is the effective mass normalized to the free electron mass ( $m_e$ ),  $T_D$  is the Dingle temperature and  $B_{MB}$  is the MB field. Integers  $t_i$  and  $b_i$  are respectively the number of tunnelling and Bragg reflections encountered along the path of the quasiparticle. Within this framework, high order harmonics of a given component are regarded as frequency combinations (since e.g.  $F_{2\alpha} = 2F_\alpha$ ), which is compatible with the semiclassical model of Falicov and Stachowiak [3,20] (which predicts  $m_{2\alpha}^* = 2m_\alpha^*$ , see below) and, in any case, has no influence on the data analysis.

The effective mass linked to each of the observed Fourier components, of which the frequencies are in the range from  $F_\alpha$  to  $F_{\beta+\alpha}$ , have been derived from the temperature dependence of their amplitude for various field windows. As an example, data are given in Figure 3 for a mean magnetic field value of 38 T. It has been checked that the values (listed in Table 1) determined for each of the considered Fourier components remain field-independent within the error bars in the range explored, in agreement with the semiclassical model. It can be remarked that  $m_\alpha^*$  and  $m_\beta^*$  are very low. Indeed, to our knowledge, the lowest effective

masses reported up to now for a linear chain of orbits were observed in (BEDO-TTF)<sub>5</sub>[CsHg(SCN)<sub>4</sub>]<sub>2</sub> [19] for which  $m_\alpha^* = 1.6 \pm 0.1$  and  $m_\beta^* = 3.0 \pm 0.3$ . In any case, the measured effective masses are much lower than in the case of  $\kappa$ -(BEDT-TTF)<sub>2</sub>Cu(NCS)<sub>2</sub> for which  $m_\alpha^* = 3.5 \pm 0.1$  and  $m_\beta^* = 7.1 \pm 0.5$  [5].

According to the coupled network model of Falicov and Stachowiak [3,20], the effective mass value of a given MB orbit is the sum of the effective masses linked to each of the FS pieces constituting the considered orbit. Oppositely, in the framework of the QI model [21], the effective mass linked to a quantum interferometer is given by the absolute value of the difference between the effective masses linked to each of its two arms. This leads, in the present case, to:

$$m_{k\beta \pm l\alpha}^* = |k \times m_\beta^* \pm l \times m_\alpha^*| \quad (5)$$

for MB orbits or QI paths. Oppositely, analytical calculations of the effective masses related to the frequency combinations induced by the oscillation of the chemical potential in dHvA spectra of an ideal two-band electronic system yield [22]:

$$m_{k\beta \pm l\alpha}^* = k \times m_\beta^* + l \times m_\alpha^* \quad (6)$$

which is at variance with the above mentioned predictions for QI paths. The failure of Eq. 5 in order to account for the effective mass of the 2<sup>nd</sup> harmonics of  $\alpha$  has been reported for many 2D compounds [23]. In contrast, Eq. 5

is in full agreement with the data of  $2\alpha$  (see Table 1) as it has already been reported for the  $2\alpha$  [5,24] and  $2\beta$  [25] components observed in magnetoresistance data of other linear chains of orbits. However, according to the data of Table 1, neither Eq. 5, nor Eq. 6 (which, strictly speaking, is relevant only for dHvA spectra) account for the effective mass of  $\beta - \alpha$ . This result is at variance with the magnetoresistance data of Refs. [5,19,25] for which Eq. 5 holds<sup>2</sup>. Oppositely, Eq. 5 accounts for the effective mass of  $\beta - 2\alpha$ , as already observed for other compounds [6,19]. As for  $\beta + \alpha$ , the effective mass reported in Table 1 is slightly, although definitely, higher than the value predicted by Eq. 5. Discrepancies between magnetoresistance data relevant to the MB orbits and the predictions of the Falicov-Stachowiak model are also reported for several other compounds with similar FS [5].

These puzzling behaviours can be further checked by considering the field dependence of the various component's amplitude. According to Eqs. 1-4, their temperature-independent part is given by:

$$\frac{A_i}{R_{Ti}} \propto \exp\left[-\frac{\alpha T_D m_i^* + t_i B_{MB}/2}{B}\right] \times \left[1 - \exp\left(-\frac{B_{MB}}{B}\right)\right]^{\frac{b_i}{2}} \quad (7)$$

The field dependence of this parameter is reported in Figure 4 for most of the Fourier components considered in Figure 3. It can be remarked first that, as expected

<sup>2</sup> DHvA data of Refs. [8,9] yield large effective masses for  $\beta - \alpha$ , although lower than predicted by Eq. 6.

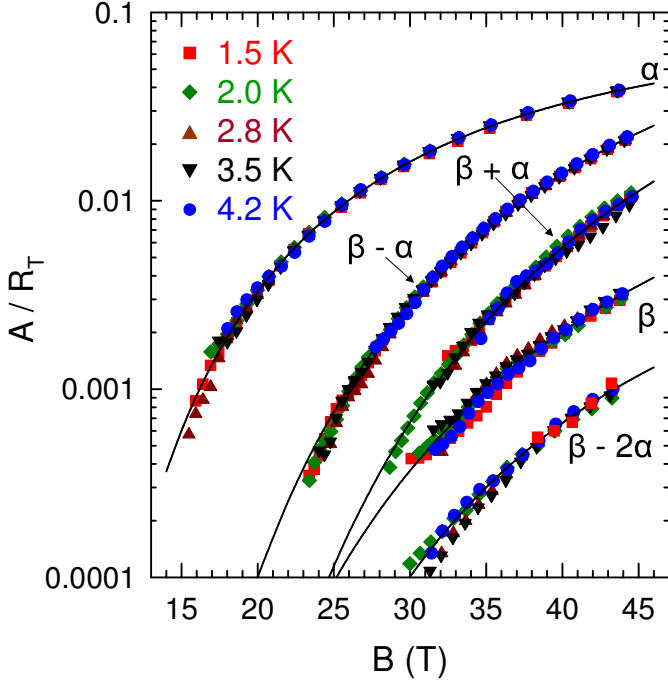


**Fig. 4.** Field dependence of the temperature-independent part of Fourier components deduced from data in Figure 2.  $A$  and  $R_T$  are the amplitude and the thermal damping factor of the considered Fourier component, respectively. Solid lines are best fits of Eq. 1 to the data.

from Eq. 7, the measured values of  $A_i / R_{Ti}$  are actually temperature-independent in the range explored whatever the considered Fourier component is. An estimation of  $T_D$  can be derived from the data of Fourier components for which  $t_i = 0$ . Assuming a low value for  $B_{MB}$ , namely  $B_{MB} \leq 2$  T, which is plausible owing to band structure calculations, data of the  $\alpha$  component yield  $T_D = (7.0 \pm 0.7)$  K [ $T_D = (7.9 \pm 0.7)$  K for crystal #2], which corresponds to a large scattering rate ( $\tau^{-1} \approx 6 \times 10^{12} \text{ s}^{-1}$ ). It must be noticed that the determined value of  $T_D$  depend on  $B_{MB}$  while the given error bars only account for the experimental noise and the uncertainty on the relevant effective mass. However, the  $B_{MB}$  sensitivity of  $T_D$

is moderate in the considered case since  $T_D = (6.7 \pm 0.7)$  K and  $(6.3 \pm 0.6)$  K, assuming  $B_{MB} = 10$  T and 30 T, respectively. These values are very close to each other and in any case equal within the error bars. As for the MB field, the parameter  $A_i / R_{Ti}$  goes to a maximum at  $B_{max} = B_{MB} / \ln[1 + b_i B_{MB} / (2\alpha m_i^* T_D + t_i B_{MB})]$ , according to Eq. 7.  $B_{max}$  should be reasonably less than the maximum field reached in the experiments in order to derive a reliable estimation of  $B_{MB}$  [4]. In the present case, the lowest value of  $B_{max}$  is obtained in the case of the  $\alpha$  component. Unfortunately, the large Dingle temperatures reported above lead to values of  $B_{max}$  much larger than the maximum field reached in the experiments, whatever the value of  $B_{MB}$  is. As a matter of fact, changing the value of  $B_{MB}$  used in the fittings of Figure 4 (which, otherwise, are obtained with  $B_{MB} = 10$  T) yields almost indiscernible curves in the magnetic field range explored. According to

Eq. 7,  $B_{MB}$  could also be derived from the data linked to the  $\beta$  component, assuming the Dingle temperature relevant for this orbit is the same as for  $\alpha$ . However, taking into account the above reported uncertainty on  $T_D$ ,  $B_{MB}$  values compatible with the data relevant for the  $\alpha$  component are in the range from 0 to 30 T which is probably valid but constitutes a very large uncertainty. Besides, the field-dependent data of Figure 4 for the components  $\beta - 2\alpha$ ,  $\beta - \alpha$  and  $\beta + \alpha$  yield values of  $T_D$  which are in poor agreement with the data for  $\alpha$  and  $\beta$ <sup>3</sup>. Remarkably, and

<sup>3</sup> For  $B_{MB} = 10$  T, the Dingle temperatures are  $(8.1 \pm 0.7)$  K,  $(5.1 \pm 0.6)$  K and dozens of K, for  $\beta - \alpha$ ,  $\beta + \alpha$  and  $\beta - 2\alpha$ , respectively.

at variance with the preceding feature, data for the harmonics  $2\alpha$  yield  $T_D = (7.1 \pm 0.7)$  K and  $T_D = (8.2 \pm 1.3)$  K for crystal #1 and #2, respectively which is in very good agreement with the data for the  $\alpha$  orbit.

Finally, the assumption of a negligibly small contribution of the chemical potential oscillation to the oscillatory data can be checked a posteriori. Indeed, according to [26], the cross-over temperature  $T_{co}$ , above which the influence of the chemical potential oscillation on the observed Fourier components of a two-band electronic system becomes insignificant, is given by  $T_{co} \simeq 3B/\alpha m^* - T_D$ . In the case of the  $\alpha$  orbit, which is the orbit with the lowest effective mass,  $T_{co}$  is equal to 1.5 K (i. e. the lowest temperature reached in the experiments) at  $B = (48 \pm 6)$  T, for crystal #1. This value lies very close to the upper boundary of the field range considered in the experiments which indicates that, in addition to QI, the only non-semiclassical phenomenon susceptible to significantly contribute to the oscillatory spectra is the coherent MB-induced modulation of the DOS [2,3,10].

## 4 Summary and conclusion

The FS of the organic metal  $(BEDO)_5Ni(CN)_4 \cdot 3C_2H_4(OH)_2$  corresponds to a linear chain of orbits coupled by MB. Oscillatory magnetoresistance spectra have been obtained in the temperature range from 1.5 to 4.2 K in magnetic fields up to 50 T. The temperature and field dependence of the Fourier components' amplitude linked to the closed  $\alpha$  and MB-induced  $\beta$  orbits, analyzed in the framework of the semiclassical model of Falicov and Stachowiak yields

consistent results. In addition, both the temperature and field dependencies of the component linked to the  $2^{nd}$  harmonics of  $\alpha$  are in good agreement with the semiclassical model (same Dingle temperature as for  $\alpha$  and twice as large effective mass). The deduced scattering rate  $\tau^{-1} \approx 6 \times 10^{12} \text{ s}^{-1}$  is very large that, according to [26], allows for considering that the contribution of the chemical potential oscillation to the oscillatory magnetoresistance spectra is negligible in the explored field and temperature ranges. Despite of this feature, the recorded spectra exhibit frequency combinations. Their effective masses and (or) Dingle temperature are not in agreement with either the predictions of the QI model or the semiclassical model of Falicov and Stachowiak. It can also be remarked that their amplitude can be very large. In particular, the amplitude of the components  $\beta - \alpha$  and  $\beta + \alpha$  is larger than that of  $\beta$ . These results suggest that additional contribution, such as the coherent MB-induced modulation of the DOS [2,3,10], can play a significant role in the observed frequency combinations.

This work was supported by the French-Spanish exchange program between CNRS and CSIC (number 16 210), Euromagnet under the European Union contract R113-CT-2004-506239, DGI-Spain (Project BFM2003-03372-C03) and by Generalitat de Catalunya (Project 2005 SGR 683). Helpful discussions with G. Rikken are acknowledged.

## References

1. R. Rousseau, M. Gener and E. Canadell, *Adv. Func. Mater.* **14**, 201 (2004).
2. A. B. Pippard, *Proc. Roy. Soc. (London)* **A270** 1 (1962).
3. D. Shoenberg, *Magnetic Oscillations in Metals* (Cambridge University Press, Cambridge, 1984).
4. D. Vignolles, A. Audouard, L. Brossard, S. I. Pesotskii, R. B. Lyubovskii, M. Nardone, E. Haanappel and R. N. Lyubovskaya, *Eur. Phys. J. B*, **31** 53 (2003); A. Audouard, D. Vignolles, E. Haanappel, I. Sheikin, R. B. Lyubovskii and R. N. Lyubovskaya, *Europhys. Lett.* **71** 783 (2005).
5. N. Harrison, J. Caulfield, J. Singleton, P. H. P. Reinders, F. Herlach, W. Hayes, M. Kurmoo and P. Day, *J. Phys. Condens. Matter* **8** 5415 (1996).
6. M.V. Kartsovnik, G. Yu. Logvenov, T. Ishiguro, W. Biberacher, H. Anzai, N.D. Kushch, *Phys. Rev. Lett.* **77** 2530 (1996).
7. F. A. Meyer, E. Steep, W. Biberacher, P. Christ, A. Lerf, A. G. M. Jansen, W. Joss, P. Wyder and K. Andres, *Europhys. Lett.* **32** 681 (1995).
8. S. Uji, M. Chaparala, S. Hill, P. S. Sandhu, J. Qualls, L. Seger and J. S. Brooks, *Synth. Met.* **85** 1573 (1997).
9. E. Steep, L. H. Nguyen, W. Biberacher, H. Müller, A. G. M. Jansen and P. Wyder, *Physica B* **259-261** 1079 (1999).
10. P. S. Sandhu, J. H. Kim and J. S. Brooks, *Phys. Rev. B* **56** (1997) 11566; J. Y. Fortin and T. Ziman, *Phys. Rev. Lett.* **80** (1998) 3117; V. M. Gvozdkov, Yu V. Pershin, E. Steep, A. G. M. Jansen and P. Wyder, *Phys. Rev. B* **65** 165102 (2002).
11. A. S. Alexandrov and A. M. Bratkovsky, *Phys. Rev. Lett.* **76** (1996) 1308; *Phys. Lett. A* **234** 53 (1997) and *Phys. Rev. B* **63** 033105 (2001); T. Champel, *ibid.* **65** 153403 (2002); K. Kishigi and Y. Hasegawa, *ibid.* **65** 205405 (2002).
12. K. Kishigi T. Ziman and H. Ohta, *Physica B* **329-333** 1156 (2003).
13. A. D. Dubrovskii, N. G. Spitsina, L. I. Buravov, G. V. Shilov, O. A. Dyachenko, E. B. Yagubskii, V. N. Laukhin and E. Canadell, *J. Mater. Chem.* **15** (2005) 1248.
14. H. Urayama, H. Yamochi, G. Saito, K. Nozawa, T. Sugano, M. Kinoshita, S. Sato, K. Oshima, A. Kawamoto and J. Tanaka, *Chem. Lett.* 55 (1988).
15. M. Schiller, W. Schmidt, E. Balthes, D. Schweitzer, H. J. Koo, M. H. Whangbo, I. Heinen, T. Klaus, P. Kircher, W. Strunz, *Europhys. Lett.* **51** 82. (2000).
16. M. Weger, M. Tittelbach, E. Balthes, D. Schweitzer and H. J. Keller, *J. Phys.: Condens. Matter* **5** 8569 (1993).
17. J. Caulfield, W. Lubczynski, F. L. Pratt, J. Singleton, D. Y. K. Ko, W. Hayes, M. Kurmoo and P. Day, *J. Phys.: Condens. Matter* **6** (1994) 2911; T. Biggs, A. K. Klehe, J. Singleton, D. Bakker, J. Symington, P. Goddard, A. Ardavan, W. Hayes, J. A. Schlueter, T. Sasaki and M. Kurmoo, *ibid.* **14** L495 (2002).
18. E. Balthes, D. Schweitzer, I. Heinen, H.J. Keller, W. Biberacher, A. G. M. Jansen, E. Steep, *Synth. Metals* **70** 841 (1995); D. Schweitzer, E. Balthes, S. Kahlich, I. Heinen, H.J. Keller, W. Strunz, W. Biberacher, A. G. M. Jansen, E. Steep, *ibid.* **70** 857 (1995).
19. R. B. Lyubovskii, S. I. Pesotskii, M. Gener, R. Rousseau, E. Canadell, J. A. A. J. Perenboom, V. I. Nizhankovskii, E. I. Zhilyaeva, O. A. Bogdanova and R. N. Lyubovskaya, *J. Mater. Chem.* **12** 483 (2002).
20. L. M. Falicov and H. Stachowiak, *Phys. Rev.* **147** 505 (1966).

21. R. W. Stark and C. B. Friedberg, *Phys. Rev. Lett.* **26** 556 (1971); R. W. Stark and C. B. Friedberg, *J. of Low Temp. Phys.* **14** 111 (1974).
22. J. Y. Fortin, E. Perez and A. Audouard, *Phys. Rev. B* **71** 155101 (2005).
23. see N. Harrison, R. Bogaerts, P. H. P. Reinders, J. Singleton, S. J. Blundell and F. Herlach, *Phys. Rev. B* **54** 9977 (1996) and references therein.
24. A. A. House, W. Lubczynski, S. J. Blundell, J. Singleton, W. Hayes, M. Kurmoo and P. Day, *J. Phys.:Condens. Matter* **8** 10377 (1996).
25. T. G. Togonidze, M. V. Kartsovnik, J. A. A. J. Perenboom, N. D. Kushch and H. Kobayashi, *Physica B* **294-295** 435 (2001).
26. K. Kishigi and Y. Hasegawa, *Synth. Met.* **153** 381 (2005).